Geophysical Research Letters

RESEARCH LETTER
10.1029/2022GL099406

**Key Points:**

- Driving mechanisms for the North Pacific subtropical mode water formation exhibit a regime shift with a periodicity of about 50–70 years
- Multidecadal regime shifts are associated with meridional and zonal shifts in the Aleutian Low (AL)
- Position shift of the AL affects the variability of the local air-sea flux and remotely driven oceanic dynamics

**Supporting Information:**

Supporting Information may be found in the online version of this article.

**Correspondence to:**

H. J. Lee,
hjlee@kmou.ac.kr

**Citation:**

Kim, S.-Y., Kwon, Y.-O., Park, W., & Lee, H. J. (2022). Multidecadal regime shifts in North Pacific subtropical mode water formation in a coupled atmosphere-ocean-sea ice model. *Geophysical Research Letters*, *49*, e2022GL099406. https://doi.org/10.1029/2022GL099406

Received 3 MAY 2022
Accepted 25 SEP 2022

**Author Contributions:**

**Conceptualization:** Sang-Yeob Kim, Young-Oh Kwon, Ho Jin Lee
**Formal analysis:** Sang-Yeob Kim
**Funding acquisition:** Ho Jin Lee
**Investigation:** Sang-Yeob Kim
**Methodology:** Sang-Yeob Kim, Young-Oh Kwon, Wonsun Park, Ho Jin Lee
**Project Administration:** Ho Jin Lee
**Software:** Sang-Yeob Kim, Young-Oh Kwon, Wonsun Park, Ho Jin Lee
**Supervision:** Ho Jin Lee
**Validation:** Sang-Yeob Kim, Young-Oh Kwon, Wonsun Park, Ho Jin Lee
**Visualization:** Sang-Yeob Kim, Young-Oh Kwon, Wonsun Park, Ho Jin Lee
**Writing – original draft:** Sang-Yeob Kim
**Writing – review & editing:** Young-Oh Kwon, Wonsun Park, Ho Jin Lee



# Multidecadal Regime Shifts in North Pacific Subtropical Mode Water Formation in a Coupled Atmosphere-Ocean-Sea Ice Model

**Sang-Yeob Kim[1], Young-Oh Kwon[2], Wonsun Park[3,4,5], and Ho Jin Lee[6]**

[1]Korea Institute of Ocean Science and Technology, Busan, South Korea, [2]Woods Hole Oceanographic Institution, Woods Hole, MA, USA, [3]GEOMAR Helmholtz Centre for Ocean Research Kiel, Kiel, Germany, [4]Center for Climate Physics, Institute for Basic Science, Busan, South Korea, [5]Department of Climate System, Pusan National University, Busan, South Korea, [6]Department of Ocean Science, Korea Maritime and Ocean University, Busan, South Korea

**Abstract** A regime shift in the formation mechanisms of the North Pacific subtropical mode water (NPSTMW) and its causes were investigated using a 2,000-year-long pre-industrial control simulation of a fully coupled atmosphere-ocean-sea ice model. The volume budget analysis revealed that the air-sea flux and ocean dynamics (OD) were the two primary driving mechanisms for NPSTMW formation, but their relative importance has periodically alternated in multidecadal timescales of approximately 50–70 years. The regime shift of the NPSTMW formation was closely related to the meridional (50 years) and zonal (70 years) movements of the Aleutian Low (AL). When AL shifted to the south or east, it induces the sea surface height anomalies propagating westward from the central North Pacific and preconditions the NPSTMW formation, thus the OD become relatively more important.

**Plain Language Summary** In the western North Pacific, a thick subsurface layer with low potential vorticity and relatively uniform potential density called the North Pacific subtropical mode water (NPSTMW) is found between depths of 100 and 400 m. Using a coupled atmosphere-ocean-sea ice model integrated over 2,000 years with constant $CO_2$ concentration at the pre-industrial level, we studied the multidecadal regime shift of the NPSTMW formation. It was found that the major driving mechanisms of NPSTMW formation periodically shifted from local atmospheric forcing to ocean dynamics (OD) (and vice versa) in approximately 50–70 years. It was also found that the multidecadal regime shifts of the NPSTMW formation are associated with the latitudinal (50 years) and longitudinal (70 years) shifts of the Aleutian Low (AL) position, that is, large (small) southward and eastward extent of the AL during the epoch when the OD (air-sea flux [ASF]) dominates. The position shift of the AL affects the variability of the local ASF and remotely driven OD via the Ekman pumping/suction.

## 1. Introduction

A thick subsurface layer with low potential vorticity (PV) and relatively uniform potential density ($\sigma_\theta = 24.8–25.7$ kg m$^{-3}$), called the North Pacific subtropical mode water (NPSTMW), exists in the northwestern Pacific (Masuzawa, 1969; Oka & Qiu, 2012). NPSTMW affects the sea surface temperature and upper-layer distribution of geochemical tracers in the following winter via the reemergence process (Alexander & Deser, 1995; Bates, 2012; Oka et al., 2019). In addition, its annual formation rate influences the occurrence of marine heatwaves in the following winter and early spring in remote areas near the dateline (Tak et al., 2021). Therefore, it is important to understand NPSTMW variability and its relationship with oceanic conditions for improving climate and extreme event predictions.

Two primary drivers controlling NPSTMW formation have been suggested: (a) local oceanic heat loss due to the air–sea interaction during cooling season (Bingham, 1992; Hanawa, 1987; Hanawa & Hoshino, 1988) and (b) changes in stratification in NPSTMW formation area driven by the propagating Rossby wave (Cerovečki & Giglio, 2016; Qiu & Chen, 2006). Hanawa and Hoshino (1988) and Bingham (1992) reported that the formation of NPSTMW is closely related to the amount of oceanic heat released by local atmospheric cooling in winter. On the other hand, Qiu and Chen (2006) analyzed observational data from 1993 to 2004 and found that NPSTMW formation was increased (reduced) when the Kuroshio Extension (KE) was stable (unstable). Cerovečki and Giglio (2016) showed from Argo data in 2005–2012 that pycnocline depth anomalies in the central North Pacific

propagated into the KE region and changed the stratification fields to determine the volume of NPSTMW formed in winter.

The regime shift in main driver of NPSTMW formation was pointed out based on the observed mixed layer data (Iwamaru et al., 2010; Sugimoto & Kako, 2016): from local air-sea interaction before the late-1980s to ocean dynamics (OD) including vertical entrainment. Kim et al. (2020) also detected the regime shift in the driving mechanism of NPSTMW formation around the late-1980s using a 50-year (1960–2009) ocean model hindcast simulation. They suggested that the regime shift of NPSTMW formation was caused by wind stress curl changes in the central North Pacific since the late-1980s, which seems to be related to the eastward shift of the North Pacific Oscillation (NPO). However, the study period was too short to reveal whether the regime shift is periodic and what drives such multidecadal variability in NPSTMW formation.

Changes in the leading modes of atmospheric circulation variability in the North Pacific are reported by multiple studies. Pak et al. (2014) showed that the correlation between the East Asian winter monsoon and the NPO significantly decreased after the late-1980s, probably due to the eastward movement of the NPO. Yeh et al. (2018) showed that the center of the southern lobe of the NPO significantly shifted to the east after the mid-1990s. Sugimoto and Hanawa (2009) analyzed reanalysis data from 1950 to 2006 and reported that there is decadal and interdecadal variability in the latitudinal and longitudinal position of the Aleutian Low (AL) with the former causing changes in the wind stress curl and the baroclinic Rossby wave in the central North Pacific, affecting the upper oceanic condition in the KE.

Here, we investigate the multidecadal regime shifts in NPSTMW formation using a 2000-year-long pre-industrial control simulation of a climate model. The purpose of this study is to investigate (a) whether the regime shift of the NPSTMW formation is periodic and (b) what drives the regime shift of the NPSTMW formation. The use of long-term simulation is expected to provide information complementary to previous studies based on limited observational data. It should be noted that the "regime shift" is used in this study to indicate a transition of driving mechanisms for NPSTMW formation, rather than abrupt changes in the mean state in the climate system.

The remainder of this paper is organized as follows: Section 2 describes the model simulation, supporting observational data, and methodology used in this study. Section 3 explains results from the analyses of multidecadal regime shifts of NPSTMW formation. Finally, Section 4 summarizes the study.

## 2. Data and Methods

We analyzed a multimillennial control integration using a fully coupled atmosphere-ocean-sea ice model, the Kiel Climate Model (KCM, Park et al., 2009; Text S1 in Supporting Information S1). We applied pre-industrial constant concentration of greenhouse gases (e.g., $CO_2$ concentration of 286.2 ppm) and initial conditions are taken from the observed climatology of temperature and salinity (Levitus, 1998). We analyzed the last 2,000 years after skipping the initial 1,000 years to consider the adjustment period. The performance of KCM was validated using the observed data (Figure S1 in Supporting Information S1). The KCM reproduces well the Kuroshio system, winter mixed layer depth (MLD) and the low PV water, although there is a limitation of non-eddy resolving model (e.g., Kuroshio overshooting). Details on comparison of model and observation are presented in supporting information (Text S2 in Supporting Information S1).

We defined NPSTMW as low PV ($<1.5 \times 10^{-10}$ m$^{-1}$ s$^{-1}$) water with a density ($\sigma_\theta$) range of 24.6–25.2 kg m$^{-3}$. PV was defined as:

$$\mathrm{PV} = -\frac{f}{\rho_0}\frac{\partial \rho}{\partial z} \tag{1}$$

where $f$ is the Coriolis parameter and $\rho_0$ and $\rho$ are the mean (1,025 kg m$^{-3}$) and anomalous potential densities of the seawater, respectively. The minimum thickness of NPSTMW was set to 50 m, as suggested by Douglass et al. (2012), to avoid the thin surface mixed layer, although this criterion may also exclude subsurface portion of NPSTMW near its lateral boundaries. Because NPSTMW is mainly formed south of the KE (Masuzawa, 1969; Oka & Qiu, 2012; Rainville et al., 2014), we considered the area from 137 to 157°E and 29 to 37°N as our study region (box in Figure S1b in Supporting Information S1).

To quantitatively analyze how NPSTMW forms during cooling seasons, the volume budget of NPSTMW was analyzed based on the Walin framework (Walin, 1982). Following Kim et al. (2020), the conservation equation for a control volume ($V$) bounded by $\sigma_1$ and $\sigma_2$ isopycnals (24.6 and 25.2 kg m$^{-3}$ in this study, respectively) can be obtained as:

$$\frac{\partial V}{\partial t} = \int_{\sigma_1}^{\sigma_2} \left[ -\frac{\partial}{\partial \sigma} \iint_{\text{outcrop}_{\text{surf}}} -\frac{\alpha Q}{c_p} + \beta \rho S(E-P) \mathrm{d}A_{\text{surf}} \right] \mathrm{d}\sigma - \iint_{\text{outcrop}_{\text{ml}}} \left( -\frac{\partial h}{\partial t} - U_h \cdot \nabla h - w_h \right) \mathrm{d}A_{ml} - \iint \mathbf{u} \cdot \boldsymbol{n} \, \mathrm{dA}_{\text{lateral}} + \mathrm{V}_{\text{residual}} \quad (2)$$

where $\alpha$ and $\beta$ are the thermal expansion and saline contraction coefficients; $c_p$ is the specific heat of seawater; $Q$ is the net surface heat flux (positive for ocean heat gain); $\rho$ is the sea surface density; $S$ is the sea surface salinity; $E$ and $P$ are the evaporation and precipitation, respectively; $A_{\text{surf}}$ is the outcrop surface area between $\sigma_1$ and $\sigma_2$ isopycnals; $h$ is the MLD; $U_h$ and $w_h$ are the lateral and vertical velocities at the base of the mixed layer; $A_{\text{ml}}$ is the area for the density range between $\sigma_1$ and $\sigma_2$ at the base of the mixed layer; $\mathbf{u}$ is the horizontal velocity within the mixed layer; $\boldsymbol{n}$ is the normal unit vector of the lateral boundary (outward positive); $A_{\text{lateral}}$ is the element of the area between $\sigma_1$ and $\sigma_2$ isopycnals at the lateral open boundaries of the analysis domain; and $V_{\text{residual}}$ is the residual term representing processes that are not considered here explicitly, such as diapycnal diffusive flux. The local eddy effect on NPSTMW formation suggested by Qiu and Chen (2006) was not considered in this study because the eddy activity in the KE region cannot be reproduced realistically in the non-eddy-resolving (~0.5°) model. We note that the second term on the right-hand-side of Equation 2 is mainly controlled by the temporal MLD change ($\partial h/\partial t$) (not shown).

We defined MLD as the thickness of the mixed layer where the vertical density gradient ($-\frac{\partial \rho}{\partial z}$) is less than $2.0 \times 10^{-3}$ kg m$^{-4}$, which is consistent with the criterion of PV ($1.5 \times 10^{-10}$ m$^{-1}$ s$^{-1}$) for NPSTMW. We followed Nishikawa and Kubokawa (2012)'s definition of the MLD, which is more suitable to detect low PV water. The left-hand side of Equation 2 is the temporal change in NPSTMW volume. The right-hand side terms represent the surface transformation rate, vertical entrainment/detrainment rate, and advective volume flux through the lateral boundaries of the domain, respectively. The volume indicates the "newly formed NPSTMW volume" within the mixed layer because the criteria of density and MLD in Equation 2 satisfy NPSTMW definitions of density and PV.

To focus on NPSTMW formation, Equation 2 was integrated over the entire cooling season (from December to March; DJFM) when $\partial V/\partial t$ was positive (i.e., when the control volume increased). We named the three terms on the right-hand side of Equation 2 as ASF, ENT (entrainment), and ADV (advection), which represent the ASF, vertical entrainment, and advective flux, respectively.

The statistical significance of the linear regression and correlation coefficient were estimated using the bootstrap method (Von Storch & Zwiers, 1999) with 1,000 resamples and a random permutation (1,000 times) method of time series in frequency domain (Ebisuzaki, 1997). A moving correlation analysis was conducted to examine decadal changes in the interannual relationship between NPSTMW volume and volume budget terms. The bootstrap method was applied to each time segment to determine the statistical significance of the moving correlation. To examine the statistical significance of the differences between the two samples, we adopted the Mann-Whitney-Wilcoxon test, which is a nonparametric test (Mann & Whitney, 1947) suitable for testing the distribution of elements in samples that are not normally distributed.

## 3. Results

To identify the key parameters driving NPSTMW formation during winter, we estimate the volume budget using Equation 2. The results show that the ENT term dominates formation during winter, averaging $2.04 \times 10^{14}$ m$^3$ (Figure 1a). While ASF ($0.51 \times 10^{14}$ m$^3$) is the second-largest term, ADV shows a net outflow mainly through the eastern and southern lateral boundaries ($-0.45 \times 10^{14}$ m$^3$). The average of the residual term is approximately $0.16 \times 10^{14}$ m$^3$, which represents neglected terms, such as the diapycnal diffusive flux. NPSTMW volume in March (not shown) and the newly formed volume integrated over DJFM (black line) exhibit almost identical temporal variability ($r = 0.99$), with time mean values of $2.26 \times 10^{14}$ m$^3$. Therefore, we use the DJFM integration of the left-hand side of Equation 2 to represent the volume in March as well as the newly formed volume in winter in the subsequent analyses and call it as total formation or volume time series. We group the formation terms in Equation 2 into two terms: local ASF and OD, with the latter combining ENT and ADV.

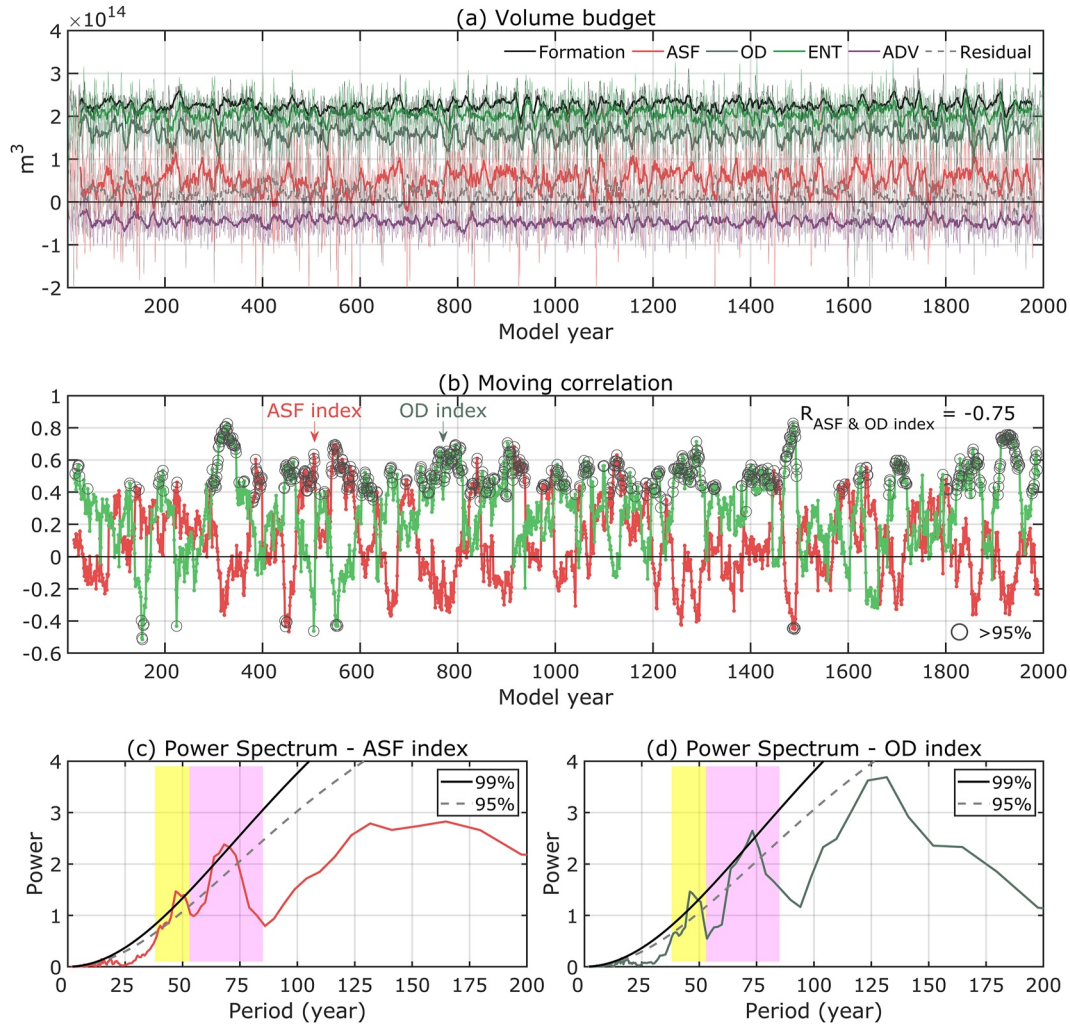


**Figure 1.** (a) Time series of the volume budget terms in Equation 2. Volume budget terms integrated during cooling season (DJFM) include the total volume formation (black), air-sea flux (ASF, red), vertical entrainment (ENT, green), advection (ADV, purple), and residual (dashed gray) terms. The sum of ENT and ADV is called the ocean dynamics (OD, dark green). (b) The 25-year moving correlation coefficients between the total volume formation term and the ASF term (red, this moving correlation time series is termed ASF index) or OD term (light green, OD index). Open circles indicate significant correlation coefficients at the 95% confidence level. The 25-year moving correlation is the correlation between two time series within the window of ±12 years relative to the corresponding year. Power spectra of the (c) ASF and (d) OD indices from (b). Solid and dashed black lines indicate statistical significance at 99% and 95%, respectively. The yellow and pink shadings denote the 38–53 and 53–85 years bands for filtering, respectively.

To find the main driver of the variability in NPSTMW formation and its temporal variation, we calculate the moving correlation coefficients between the total formation and the individual formation term in Equation 2 (Figure 1b). Considering the interannual to decadal variability of the volume budget terms, the moving window size is set to 25-year. Note that the results are robust, regardless of the moving window length from 17 to 33 years. We define the two-time series of moving correlation coefficients as the ASF and OD indices (i.e., $r_{\text{ASF\_NPSTMWformation}}$ and $r_{\text{OD\_NPSTMWformation}}$), respectively.

Notably, the OD index (which was dominated by ENT) and ASF index alternate being the dominant drivers for different multidecadal periods (Figure 1b). For example, the OD index exhibits a strong correlation (green curve) with NPSTMW formation from years 300–350 while the ASF index shows a negligible correlation (red curve). However, from years, 370–400, these correlations are reversed. The alternating transitions between the two drivers occur routinely throughout the record such that the two indices have a negative correlation ($r = -0.75$)

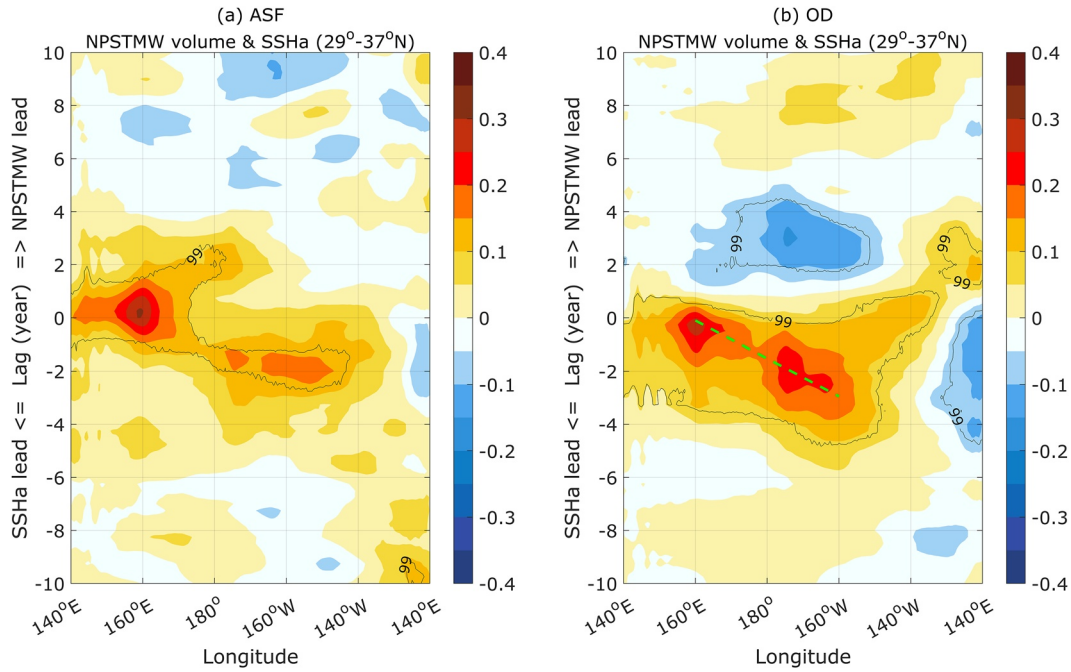


**Figure 2.** Lagged correlations between the seasonal anomalies (JFM, AMJ, JAS, and OND) of the sea surface height anomalies at different longitudes and the DJFM North Pacific subtropical mode water (NPSTMW) volume during (a) air-sea flux (ASF) and (b) ocean dynamics (OD) periods, respectively. The ASF and OD periods are defined as the years when the moving correlation coefficients in Figure 1b are higher than 0.4, that is, statistically significant at 95% confidence level. The SSH was meridionally averaged over the latitudinal band of 29–37°N. The negative lag means the SSH anomalies leading the NPSTMW volume. Black contour indicates significant correlation coefficient at the 99% confidence level.

significant at the 95% confidence level. This result suggests that the observed sudden change in the driving mechanism for NPSTMW formation in the late-1980s (Kim et al., 2020) may not be an isolated event.

To investigate the difference between the two drivers of NPSTMW formation, we compare the lagged correlation between the NPSTMW volume and sea surface height anomalies (SSHa) at different longitudes along the latitudinal band of 29–37°N for the ASF and OD dominated periods, respectively (Figure 2). Correlation patterns show a marked contrast between the two periods. In the OD period, the tilted band of positive correlation extends from 160°W at lag = −3 years to 160°E at lag = 0 year indicating that the westward propagation of SSHa driven by remote forcing can precondition NPSTMW volume changes in the western North Pacific. Westward propagation speed of the Rossby wave is about 3.9 cm/s (green dashed line). It is consistent with the previous phase speed estimated from the satellite-based observations by Qiu and Chen (2005) (∼3.7 cm/s) at the latitude 35°N. Whereas, in the ASF period, NPSTMW volume is highly correlated with the local SSHa at zero lag without a clear signal of westward propagation from the central North Pacific, although there is a statistically significant correlation in the east of 180° at lag = −2 years that is not examined in this study. This result implies the local atmospheric forcing drives NPSTMW formation during the period. This result is consistent with Kim et al. (2020) who showed the remote change of isopycnal layer thickness triggered by wind stress curl in the central North Pacific propagates into NPSTMW formation region, thus driving NPSTMW volume changes in the OD period.

The power spectrum analysis of each index shows two dominant peaks at approximately 50 and 70 years (Figures 1c and 1d), suggesting that the controlling factor for NPSTMW formation changes on multidecadal timescales. To focus on the two multidecadal regime shifts in NPSTMW formation, we applied Butterworth bandpass filters for 38–53 and 53–85 years to the OD and ASF indices, respectively, for subsequent analyses. Note that 38, 53, and 85 years correspond to the minima neighboring the maximum peaks and the results are robust regardless of the exact width of the windows between 35–55 years and 55–95 years for filtering.

We regress the sea level pressure (SLP) anomalies on the bandpass filtered OD index to examine the atmospheric conditions associated with the multidecadal regime shift of NPSTMW formation (Figure 3). Note that the regression on the ASF index has a similar pattern but the opposite sign compared to that of the regression on the OD

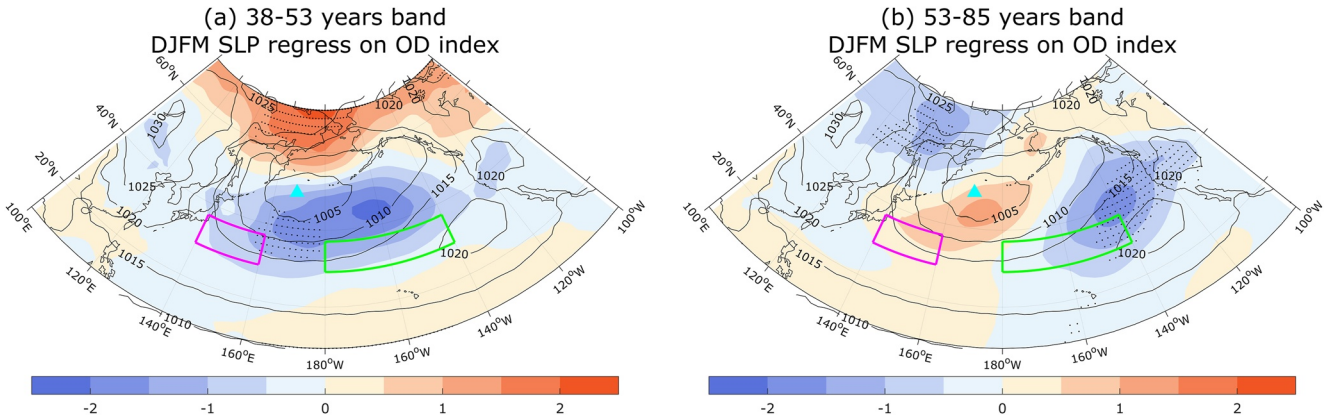


**Figure 3.** Regression map of anomalous winter (DJFM) sea level pressure (SLP) on (a) 38–53 and (b) 53–85 years band-pass filtered ocean dynamics index. Black dots indicate regions where the regression coefficients are statistically significant at the 90% confidence level. Black contours and cyan triangles denote the climatological mean DJFM SLP and the locations of the Aleutian Low center, respectively. Magenta and green boxes are the domain of the northwest and central North Pacific regions, respectively.

index, as the OD and ASF indices have a significant negative correlation ($r = -0.75$, Figure 1b). The regressed SLP patterns substantially differ between the two periods: a north-south dipole-like pattern for the 38–53 years and an east-west dipole-like pattern for the 53–85 years, implying southward and eastward shifts of the AL, respectively, when OD index is positive. A similar result is obtained by the composite difference of SLP in the years when OD or ASF index values are above +1 standard deviation (Figure S3 in Supporting Information S1). Therefore, the alternating periods of the dominant OD and ASF indices (Figures 1c and 1d) are related to the multidecadal fluctuation in AL position in the north-south and east-west directions, respectively.

To quantify the variability of AL position, we track the positions of AL center for 2,000 years (Figure S4 in Supporting Information S1). The central position of the AL is defined as DJFM SLP minimum in the region of 150–150°W and 30–60°N, following Sugimoto and Hanawa (2009). The time-mean position of AL center over 2,000 model years is located at 176.5°E, 49.6°N, which is comparable to Sugimoto and Hanawa (2009)'s result (178.2°E, 51.6°N) obtained using NCEP/NCAR reanalysis data from 1950 to 2006. The time series of AL positions showed distinctive multidecadal variability at 50 years periods in the latitudinal direction and 60–80 years in the longitudinal direction (Figures S4b and S4d in Supporting Information S1). This result is consistent with the two multidecadal peaks in the OD and ASF indices (Figures 1c and 1d), which correspond to the latitudinal and longitudinal variations of AL position, respectively.

To examine how the multidecadal variability of AL position results in a multidecadal regime shift in NPSTMW formation mechanisms, we compare the amplitudes of interannual variability of atmospheric and oceanic parameters affecting NPTSMW formation for respective periods (Figure 4). For the factors impacting the amplitude of ASF variability, we examine the 25-year moving standard deviations of the surface net heat flux and wind speed averaged over the northwestern Pacific (140–160°E, 29–37°N; magenta box in Figure 3) around the NPSTMW formation region. The 25-year moving standard deviations of the Ekman pumping velocity averaged over the central North Pacific region over the same latitudinal range of the formation region (180–140°W, 29–37°N; green box in Figure 3) is considered as the remote factor modulating the amplitude of the OD variability via the baroclinic Rossby wave propagation. The box-whisker plots, separately for the epochs when OD or ASF dominated, show that the amplitudes of the interannual variability of each parameter are significantly different between the OD epochs versus ASF epochs (Figure 4). The variability of the remote forcing via Ekman pumping became stronger in the OD epochs, whereas the local heat flux variability became stronger in the ASF epochs.

Collectively, these results suggest that when the AL migrates southward or eastward, the wind stress curl variability over the central and eastern North Pacific becomes stronger, enhancing the variability of OD in the NPSTMW volume budget by modulating the thermocline depth in the NPSTMW formation region via Rossby wave propagation. On the other hand, when the AL is in a relatively westward or northward position, its influence on the local heat flux variability over the formation region strengthens; thus, the variability of the ASF term dominates.

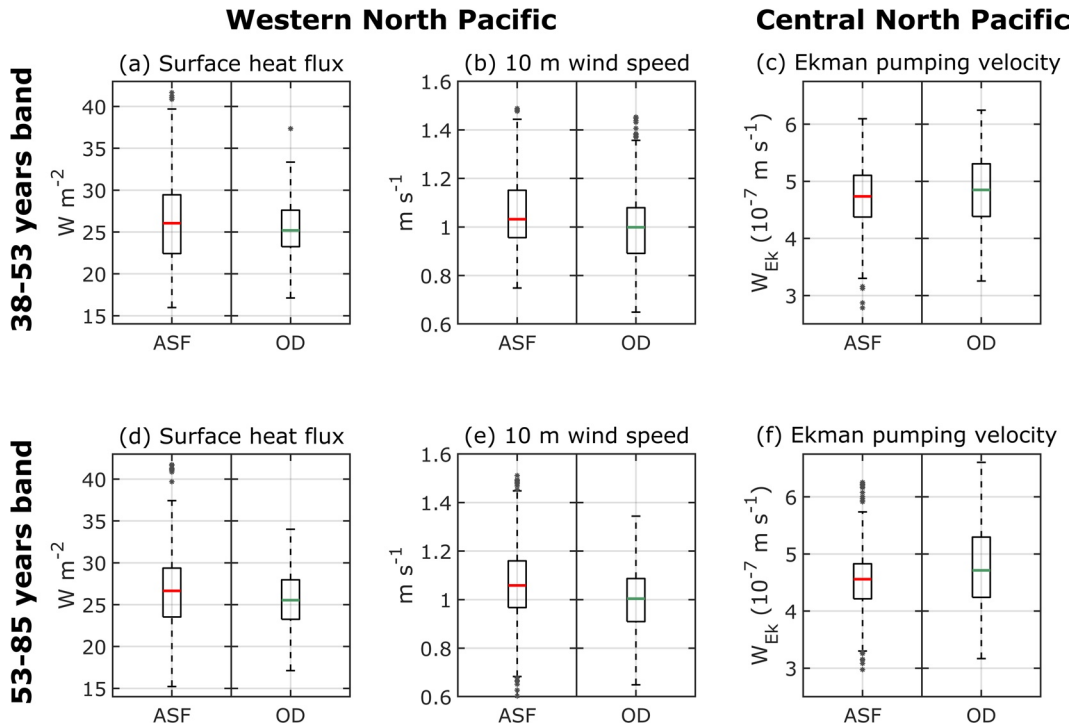


**Figure 4.** Box-and-whisker plots for 25-year moving standard deviation of anomalous winter (DJFM) (a) net surface heat flux, (b) 10 m wind speed averaged over a Northwest Pacific region (140–160°E, 29–37°N; magenta box in Figure 3), and (c) Ekman pumping velocity averaged in a central North Pacific region (180–140°W, 29–37°N; green box in Figure 3) in the air-sea flux (ASF) and ocean dynamics (OD) epochs based on the 38–53 years band-pass filtering. The solid boxes indicate 25th and 75th percentiles and thick red and green lines in the box denote the median values. The whiskers (upper and lower dashed lines) correspond to the 0.7th and 99.3rd percentiles ($\pm 2.7\sigma$) of the samples. Asterisks denote the outliers (beyond the whisker). (d–f) Same as (a–c) but for the ASF and OD epochs based on the 53–85 years band-pass filtering. The two box-whisker plots in all six panels are significantly different at 95% based on the two-sided Mann-Whitney-Wilcoxon test.

To establish a more direct link, we compared the variation in AL position between the two epochs (Figure S5 in Supporting Information S1). The latitudinal range of AL center is wider in the OD epochs than in the ASF epochs for the 38–53 years band, especially to the south of 50°N (Figure S5a in Supporting Information S1). This suggests that the interannual variability of the latitudinal position increases when the AL shifts southward. The longitudinal range of AL center does not show a clear difference between the two epochs for the 38–53 years band (Figure S5b in Supporting Information S1).

Therefore, the increased variability of the Ekman pumping in the central Pacific (180–140°W, 29–37°N) is due to wider latitudinal interannual variations in AL position (Figure S5a in Supporting Information S1) when the overall position of the AL shifts to the south in the OD epochs (Figure 3a and Figure S3a in Supporting Information S1). Ekman pumping induces a change in the thermocline depth in the central Pacific, which can propagate the disturbance into the NPSTMW formation region via a baroclinic Rossby wave and is a precondition for determining the formation volume of NPSTMW (Figure 2) (Cerovečki & Giglio, 2016; Kim et al., 2020; Qiu & Chen, 2006). Because the latitudinal variation decreases when the AL center shifted northward during the ASF, the remote effect from the central Pacific is reduced and the local heat exchange in the formation region became the main controlling factor in determining the variability of NPSTMW formation.

For the 53–85 years band, the longitudinal range in OD is slightly larger (Figure S5d in Supporting Information S1), while the latitudinal range is very similar between the two epochs (Figure S5c in Supporting Information S1). Therefore, the remote effect on the OD can be increased when AL center is shifted eastward (Figure 3b and Figure S3b in Supporting Information S1). In contrast, the westward shift of the overall AL position in the ASF epochs (Figure 3b and Figure S3b in Supporting Information S1) can increase northerly winds in the formation region by strengthening the SLP gradient between the Siberian High and the AL during winter, thereby

enhancing heat exchange through the sea surface. Indeed, the difference in the wind speed and net heat flux variability over the formation region in the ASF epoch increase for the 53–85 years band (Figures 4d and 4e).

To investigate the difference of propagation patterns of SSHa between two modes of AL position, that is, meridional and zonal modes, we estimate a lead-lag correlation between SSHa at each longitude and the NPSTMW volume for the period when the multidecadal AL anomalies for the latitude (longitude) is less (greater) than −1 (+1) standard deviation of the filtered time series, indicating that the AL position extends further south (east) (Figure S6 in Supporting Information S1). The westward propagation of the SSHa from the central North Pacific is more pronounced for the 38–53 years band-pass filtered AL meridional mode, while it is clear for the 53–85 years band-pass filtered AL zonal mode, which represent the feature of the OD epoch. This result suggests that the multidecadal period of the OD can be related with multidecadal variation of the AL position. It is notable that the propagation range is longer in the AL zonal mode, which starts from 160°W (Figure S6d in Supporting Information S1). The lag thereby is increased by a year compared with that in the AL meridional mode (Figure S6a in Supporting Information S1).

## 4. Summary and Conclusion

Multidecadal regime shift in the variability of NPSTMW formation was investigated using a 2,000-year-long control simulation of the KCM. The KCM reproduced well NPSTMW formation in the upper ocean during cooling seasons. The dominant driving mechanism of NPSTMW formation was found to be alternating on multidecadal timescales of approximately 50 and 70 years, which correspond to the multidecadal latitudinal and longitudinal fluctuations of AL position, respectively.

The interannual variability of the latitudinal position increased when AL shifted southward with a ∼50-year periodicity. The enhanced interannual variability of AL position resulted in an enhanced connection of SSHa, which reflects the thermocline depth variability, from the central North Pacific via baroclinic Rossby wave propagation, which in turn increased variability of the OD in the formation area. Therefore, the remote effect represented by the OD term in Equation 2 became more important in NPSTMW formation during this period. The OD effect can also be a controlling factor similarly when the AL center is shifted eastward with a ∼70-year periodicity.

Our findings are in line with a previous study by Kim et al. (2020) showing that a regime shift of NPSTMW formation occurred in the late-1980s. They showed that wind stress curl change in the central North Pacific driven by the eastward shift of the NPO center was responsible for the regime shift in NPSTMW formation. The 50-year (1960–2009) hindcast simulation also exhibited the changes in the Rossby wave propagation into the NPSTMW formation region in response to the meridional and zonal shifts of the AL (not shown). Using a multimillennial atmosphere-ocean-sea ice coupled model simulation, our study proposes that there could be a multidecadal regime shift in the dominant formation mechanism of NPSTMW and that such a shift may have occurred in the late-1980s.

Naturally, the cause of the multidecadal fluctuations in AL position is of interest. It may be due to either intrinsic atmospheric variability or remote forcing. In terms of remote effects, multidecadal variability related to the Atlantic Ocean was suggested to have a strong correlation with the AL (Chen et al., 2018) and the mean temperature of NPSTMW (Wu et al., 2020). Hwang et al. (2022) further reported that the eastward shift of the AL center was responsible for the weakening of the Arctic Oscillation-AL correlation, which may be related to changes in Arctic sea ice. It would be thus interesting to investigate whether and how variability in Atlantic Ocean and Arctic sea ice drives the multidecadal AL variability via an atmospheric bridge and also multidecadal regime shift of NPSTMW formation, which will be a subject of future studies. A multi-model analysis (e.g., using the CMIP simulations) also would be necessary to assess the robustness of our finding and further understand the dynamics of the multidecadal AL variability and its connection to the Atlantic Ocean and Arctic sea ice.

## Data Availability Statement

The Argo mixed-layer depth data were downloaded from http://mixedlayer.ucsd.edu. The EN4 data set was obtained from https://www.metoffice.gov.uk/hadobs/en4/. The OSCAR data were taken from https://podaac.jpl.nasa.gov/dataset/OSCAR_L4_OC_third-deg. The processed model data can be downloaded at https://doi.org/10.5281/zenodo.7118360.

**Acknowledgments**
The authors are grateful to Prof. Hyeongseog Kim in KMOU for his useful comments on statistical methods. This research was supported by the in-house projects of KIOST titled "Influences of the Northwest Pacific circulation and climate variability on the Korean water changes and material cycle I-The role of Jeju warm current and its variability" and the research project entitled "Basic Science Research Program through the National Research Foundation of Korea (NRF)" funded by the Ministry of Education, Korea (Grant NRF-2020R1A6A3A01098150). Y-OK was funded by the U.S. National Science Foundation (NSF) AGS-2040073 and NOAA MAPP NA210AR4310341. WP acknowledges support by GEOMAR and IBS (IBS-R028-D1). KCM integration was performed at the Computer Centre at the Kiel University.

## References

Alexander, M. A., & Deser, C. (1995). A mechanism for the recurrence of wintertime midlatitude SST anomalies. *Journal of Physical Oceanography*, *25*(1), 122–137. https://doi.org/10.1175/1520-0485(1995)025<0122:AMFTRO>2.0.CO;2

Bates, N. R. (2012). Multi-decadal uptake of carbon dioxide into subtropical mode water of the North Atlantic Ocean. *Biogeosciences*, *9*(7), 2649–2659. https://doi.org/10.5194/bg-9-2649-2012

Bingham, F. M. (1992). Formation and spreading of subtropical mode water in the North Pacific. *Journal of Geophysical Research*, *97*(C7), 11177–11189. https://doi.org/10.1029/92JC01001

Cerovečki, I., & Giglio, D. (2016). North Pacific subtropical mode water volume decrease in 2006–09 estimated from Argo observations: Influence of surface formation and basin-scale oceanic variability. *Journal of Climate*, *29*(6), 2177–2199. https://doi.org/10.1175/JCLI-D-15-0179.1

Chen, D., Wang, H., Sun, J., & Gao, Y. (2018). Pacific multi-decadal oscillation modulates the effect of Arctic oscillation and El Niño southern oscillation on the East Asian winter monsoon. *International Journal of Climatology*, *38*(6), 2808–2818. https://doi.org/10.1002/joc.5461

Douglass, E. M., Jayne, S. R., Peacock, S., Bryan, F. O., & Maltrud, M. E. (2012). Subtropical mode water variability in a climatologically forced model in the northwestern Pacific Ocean. *Journal of Physical Oceanography*, *42*(1), 126–140. https://doi.org/10.1175/2011JPO4513.1

Ebisuzaki, W. (1997). A method to estimate the statistical significance of a correlation when the data are serially correlated. *Journal of Climate*, *10*(9), 2147–2153. https://doi.org/10.1175/1520-0442(1997)010<2147:AMTETS>2.0.CO;2

Hanawa, K. (1987). Interannual variations of the winter-time outcrop area of subtropical mode water in the Western North Pacific ocean. *Atmosphere-Ocean*, *25*(4), 358–374. https://doi.org/10.1080/07055900.1987.9649280

Hanawa, K., & Hoshino, I. (1988). Temperature structure and mixed layer in the Kuroshio region over the Izu Ridge. *Journal of Marine Research*, *46*(4), 683–700. https://doi.org/10.1357/002224088785113397

Hwang, S.-O., Yeh, S.-W., Oh, S.-Y., & Lee, J. (2022). Recent weakening linkage between Arctic oscillation and Aleutian low during boreal winter and its impact on surface temperature over Eastern Eurasia. *Atmosphere Science Letters*, *23*(7), e1089. https://doi.org/10.1002/asl.1089

Iwamaru, H., Kobashi, F., & Iwasaka, N. (2010). Temporal variations of the winter mixed layer south of the Kuroshio Extension. *Journal of Oceanography*, *66*(1), 147–153. https://doi.org/10.1007/s10872-010-0012-1

Kim, S.-Y., Pak, G., Lee, H. J., Kwon, Y.-O., & Kim, Y. H. (2020). Late-1980s regime shift in the formation of the North Pacific subtropical mode water. *Journal of Geophysical Research: Oceans*, *125*(2), e2019JC015700. https://doi.org/10.1029/2019JC015700

Levitus, S. (1998). *NODC world ocean atlas 1998 data, report, 1998*. NOAA-CIRES Climate Diagnostic Center.

Mann, H. B., & Whitney, D. R. (1947). On a test of whether one of two random variables is stochastically larger than the other. *The Annals of Mathematical Statistics*, *18*(1), 50–60. https://doi.org/10.1214/aoms/1177730491

Masuzawa, J. (1969). Subtropical mode water. *Deep-Sea Research and Oceanographic Abstracts*, *16*(5), 463–472. https://doi.org/10.1016/0011-7471(69)90034-5

Nishikawa, S., & Kubokawa, A. (2012). Mixed layer depth front and subduction of low potential vorticity water under seasonal forcings in an idealized OGCM. *Journal of Oceanography*, *68*(1), 53–62. https://doi.org/10.1007/s10872-011-0086-4

Oka, E., & Qiu, B. (2012). Progress of North Pacific mode water research in the past decade. *Journal of Oceanography*, *68*(1), 5–20. https://doi.org/10.1007/s10872-011-0032-5

Oka, E., Yamada, K., Sasano, D., Enyo, K., Nakano, T., & Ishii, M. (2019). Remotely forced decadal physical and biogeochemical variability of North Pacific subtropical mode water over the last 40 years. *Geophysical Research Letters*, *46*(3), 1555–1561. https://doi.org/10.1029/2018GL081330

Pak, G., Park, Y.-H., Vivier, F., Kwon, Y.-O., & Chang, K.-I. (2014). Regime-dependent nonstationary relationship between the East Asian winter monsoon and North Pacific oscillation. *Journal of Climate*, *27*(21), 8185–8204. https://doi.org/10.1175/JCLI-D-13-00500.1

Park, W., Keenlyside, N., Latif, M., Ströh, A. R., Redler, E., Roeckner, R., & Madec, G. (2009). Tropical Pacific climate and its response to global warming in the Kiel Climate Model. *Journal of Climate*, *22*(1), 71–92. https://doi.org/10.1175/2008jcli2261.1

Qiu, B., & Chen, S. (2005). Variability of the Kuroshio Extension jet, recirculation gyre, and mesoscale eddies on decadal time scales. *Journal of Physical Oceanography*, *35*(11), 2090–2103. https://doi.org/10.1175/JPO2807.1

Qiu, B., & Chen, S. (2006). Decadal variability in the formation of the North Pacific subtropical mode water: Oceanic versus atmospheric control. *Journal of Physical Oceanography*, *36*(7), 1365–1380. https://doi.org/10.1175/JPO2918.1

Rainville, L., Jayne, S. R., & Cronin, M. F. (2014). Variations of the North Pacific subtropical mode water from direct observations. *Journal of Climate*, *27*(8), 2842–2860. https://doi.org/10.1175/JCLI-D-13-00227.1

Sugimoto, S., & Hanawa, K. (2009). Decadal and interdecadal variations of the Aleutian Low activity and their relation to upper oceanic variations over the North Pacific. *Journal of the Meteorological Society of Japan*, *87*(4), 601–614. https://doi.org/10.2151/jmsj.87.601

Sugimoto, S., & Kako, S. (2016). Decadal variation in winter mixed layer depth south of the Kuroshio Extension and its influence on winter mixed layer temperature. *Journal of Climate*, *29*(3), 1237–1252. https://doi.org/10.1175/JCLI-D-15-0206.1

Tak, Y.-J., Song, H., & Cho, Y.-K. (2021). Impact of the reemergence of North Pacific subtropical mode water on the multi-year modulation of marine heatwaves in the North Pacific Ocean during winter and early spring. *Environmental Research Letters*, *16*(7), 074036. https://doi.org/10.1088/1748-9326/ac0cad

Von Storch, H., & Zwiers, F. W. (1999). *Statistical analysis in climate research* (p. 494). Cambridge University Press.

Walin, G. (1982). On the relation between sea surface heat flow and thermal circulation in the ocean. *Tellus*, *34*(2), 187–195. https://doi.org/10.3402/tellusa.v34i2.10801

Wu, B., Xiaopei, L., & Yu, L. (2020). North Pacific subtropical mode water is controlled by the Atlantic multidecadal variability. *Nature Climate Change*, *10*(3), 238–243. https://doi.org/10.1038/s41558-020-0692-5

Yeh, S.-W., Yi, D.-W., Sung, M.-K., & Kim, Y. H. (2018). An eastward shift of the North Pacific oscillation after the mid-1990s and its relationship with ENSO. *Geophysical Research Letters*, *45*(13), 6654–6660. https://doi.org/10.1029/2018GL078671

## References From the Supporting Information

Alexander, M. A., Deser, C., & Timlin, M. S. (1999). The reemergence of SST anomalies in the North Pacific Ocean. *Journal of Climate*, *12*(8), 2419–2433. https://doi.org/10.1175/1520-0442(1999)012<2419:TROSAI>2.0.CO;2

Choi, H. Y., Lee, H. J., Kim, S.-Y., & Park, W. (2020). Deepening of future Aleutian low in ensemble global warming simulations with the Kiel Climate Model. *Ocean Science Journal*, *55*(2), 219–230. https://doi.org/10.1007/s12601-020-0017-7

de Boyer Montégut, C., Madec, G., Fischer, A. S., Lazar, A., & Iudicone, D. (2004). Mixed layer depth over the global ocean: An examination of profile data and a profile-based climatology. *Journal of Geophysical Research*, *109*(C12), C12003. https://doi.org/10.1029/2004JC002378

Good, S. A., Martin, M. J., & Rayner, N. A. (2013). EN4: Quality controlled ocean temperature and salinity profiles and monthly objective analyses with uncertainty estimates. *Journal of Geophysical Research: Oceans*, *118*(12), 6704–6716. https://doi.org/10.1002/2013JC009067

Holte, J., Talley, L. D., Gilson, J., & Roemmich, D. (2017). An Argo mixed layer climatology and database. *Geophysical Research Letters*, *44*(11), 5618–5626. https://doi.org/10.1002/2017GL073426

Locarnini, R. A., Misonov, A. V., Antonov, J. I., Boyer, T. P., Garcia, H. E., Baranova, O. K., et al. (2010). NOAA atlas NESDIS. In S. Levitus (Ed.), *World ocean atlas 2009, vol. 1, temperature* (Vol. 69, p. 184). NOAA.

Mizuno, K., & White, W. B. (1983). Annual and interannual variability in the Kuroshio current system. *Journal of Physical Oceanography*, *13*(10), 1847–1867. https://doi.org/10.1175/1520-0485(1983)013<1847:AAIVIT>2.0.CO;2

Sugimoto, S., & Hanawa, K. (2005). Remote reemergence areas of winter sea surface temperature anomalies in the North Pacific. *Geophysical Research Letters*, *32*(1), L01606. https://doi.org/10.1029/2004gl021410

Xu, L., Xie, S.-P., McClean, J. L., Liu, Q., & Sasaki, H. (2014). Mesoscale eddy effects on the subduction of North Pacific mode waters. *Journal of Geophysical Research: Oceans*, *119*(8), 4867–4886. https://doi.org/10.1002/2014JC009861